



SPE 159923

A Petrophysical Model To Estimate Relative and Effective Permeabilities in Hydrocarbon Systems and To Predict Ratios of Water to Hydrocarbon Productivity

Michael Holmes, SPE, Antony Holmes and Dominic Holmes, Digital Formation

Copyright 2012, Society of Petroleum Engineers

This paper was prepared for presentation at the SPE Annual Technical Conference and Exhibition held in San Antonio, Texas, USA, 8-10 October 2012.

This paper was selected for presentation by an SPE program committee following review of information contained in an abstract submitted by the author(s). Contents of the paper have not been reviewed by the Society of Petroleum Engineers and are subject to correction by the author(s). The material does not necessarily reflect any position of the Society of Petroleum Engineers, its officers, or members. Electronic reproduction, distribution, or storage of any part of this paper without the written consent of the Society of Petroleum Engineers is prohibited. Permission to reproduce in print is restricted to an abstract of not more than 300 words; illustrations may not be copied. The abstract must contain conspicuous acknowledgment of SPE copyright.

Abstract

Permeability estimates from petrophysical interpretations rely mostly on relations between porosity and irreducible water saturation, for example using the approach developed by Timur (1968). If core data are available for calibration, it is common that the transform used can be quite reliable. However, relative permeability estimates require quantification of water saturation greater than irreducible saturation.

In a previous publication by the authors, methodology was presented to distinguish rocks at irreducible saturation from those that contain mobile water. The technique involves a modified interpretation of porosity/saturation cross plots, to identify levels at irreducible water saturation using a Buckles (1965) relationship. Once this data trend has been identified, water saturation at any given data point can be compared with theoretical irreducible saturation. Values of water saturation above irreducible water saturation indicate the presence of mobile water.

Using a representative relative permeability curve, or a reservoir-specific relative permeability curve, relations can be established between water saturations above irreducible and the accompanying relative permeability, both to hydrocarbons and water. Once this is available, effective permeabilities to each phase can be calculated level-by-level. The procedure involves comparing differences between water saturation and irreducible water saturation with measured relative permeabilities to both wetting and non-wetting phases, expressed as exponential equations. Effective permeabilities are then available as the product of relative permeability and log estimated permeability. By factoring in mobility ratios of hydrocarbons and water, it is then possible to estimate profiles of water cuts in oil/water systems, or barrels of water per million cubic feet of gas (Bbl/MMCFG) in gas/water systems.

Examples are presented for both oil/water and gas/water systems, showing good correlation with fluid production from well tests.

Introduction

Standard petrophysical approaches to estimate permeability mostly rely on relations between porosity (ϕ) and irreducible water saturation (S_{wi}) – for example, the Timur equation (1968). In order to estimate relative permeability (k_r) it is necessary to consider the entire range of water saturation (S_w). Holmes, et al (2009) described a methodology to distinguish rocks at S_{wi} from those that contain mobile water. The concepts presented here extend this methodology to derive continuous depth curves of relative and effective permeabilities, in order to estimate water cut in oil-bearing reservoirs, and volumes of water produced in gas reservoirs. For this paper, only water-wet reservoirs are considered. References to k_r , are defined as wetting or water phase (k_{rw}), and oil or gas hydrocarbon wetting phase (k_{rh}). Similar references apply to effective wetting and hydrocarbon permeabilities (k_w and k_h).

Statement of Theory and Definitions

Burdine, et al (1950) related k_r to both wetting and non-wetting phase, using capillary pressure curves and tortuosity ratios based on comparisons of S_w with S_{wi} . Buckles (1965) suggested that for any singular rock type, the relationship shown in Eq.1 applies,

$$\phi \times S_{wi} = \text{Constant} \dots \dots \dots (1)$$

When Eq. 1 is true, a cross plot of $\log \phi$ vs. $\log S_{wi}$ will have a straight line, with a negative slope of unity, shown in **Fig. 1**.

Holmes, et al (2009) suggested that many reservoirs show correlations at S_{wi} with slopes on the $\log \phi$ vs. $\log S_{wi}$ plots that diverge from unity as shown in **Fig. 2**. Therefore, the Buckles (1965) relation (Eq. 1) can be amended to:

$$\phi^Q \times S_{wi} = \text{Constant} \dots\dots\dots(2)$$

The exponent Q is generally in the range of 0.8 to 1.4. Levels where S_w is greater than S_{wi} indicates the presence of mobile water, and data points will fall to the upper right of the irreducible correlation line as shown in **Fig. 3**. At each level in the reservoir, actual S_w can be compared with theoretical S_{wi} .

Calculations of ϕ and S_w are made using standard petrophysical techniques. Estimates of k are derived by combining ϕ and S_w . Cross plots of ϕ and S_w are interpreted to define S_{wi} correlations, and to quantify, level-by-level, S_w and theoretical S_{wi} . These saturation differences can then be related to specific measured k_r curves, to define depth profiles of k_r to both wetting and non-wetting phases. By incorporating in-situ viscosity values of each fluid, estimates can be made of relative mobility to wetting and non-wetting phases.

Description of Processes

Following calculations of ϕ and S_w using standard petrophysical analysis, k is calculated using a Schlumberger adaptation of the Timur equation

$$k = \frac{62500 \times \phi^6}{S_{wi}^2} \dots\dots\dots(3)$$

An initial estimate of S_{wi} is made by applying a Buckles constant for the zone under investigation. Then, the lower of \log calculated S_w or theoretical S_{wi} is applied. The Buckles constant and porosity exponent can be adjusted to match with core data, if available. A reasonable starting estimate for the Buckles constant is 0.05. $\log S_w$ vs. $\log \phi$ cross plots are then interpreted zone-by-zone to define the S_{wi} correlation stated in Eq. 2.

Then, for each level, theoretical S_{wi} and actual S_w are available. Care should be taken to incorporate, within any one zone, similar rock types with similar ϕ vs. S_{wi} relations.

A measured k_r data set, appropriate to the reservoir under consideration, is used to relate differences between S_w and S_{wi} to k_r . An example of the k_r curve from Craft and Hawkins (1959) is shown in **Fig. 4**. Using average S_{wi} values for the reservoir of interest, it is then possible to construct a table relating differences ($S_w - S_{wi}$) to \log measured S_w . A graphical solution, comparing linear $S_w - S_{wi}$ differences $\log k_r$ yields the following equations:

$$k_{rh} = 0.9e^{-5(S_w - S_{wi})} \dots\dots\dots(4)$$

when $S_w - S_{wi} < 0.45$,

$$k_{rh} = 95e^{-15.35(S_w - S_{wi})} \dots\dots\dots(5)$$

when $S_w - S_{wi} > 0.45$,

$$k_{rw} = 0.049e^{3.84(S_w - S_{wi})} \dots\dots\dots(6)$$

when $S_w - S_{wi} > 0.33$, and

$$k_{rw} = 0.002e^{13.16(S_w - S_{wi})} \dots\dots\dots(7)$$

when $S_w - S_{wi} < 0.33$

Using these equations, continuous curves of k_r to both wetting and non-wetting are available. Relative permeabilities can then be combined with absolute k to yield k_w and k_h .

For oil reservoirs, it is then possible to estimate ratios of oil to water at each level using the following equation,

$$\text{Oil:Water} = \frac{k_{rh}}{\text{oil viscosity}} \times \frac{\text{water viscosity}}{k_{rw}} \dots\dots\dots(8)$$

For gas reservoirs, the gas formation volume factor (B_g , RCF/SCF) is incorporated, and volume of water (Bbl/MMCFG) is estimated.

$$\text{Reservoir Volume MMCFG} = 1,000,000 \times B_g \dots\dots\dots(9)$$

$$\text{Gas: Water} = \frac{k_{rh}}{\text{gas viscosity}} \times \frac{\text{water viscosity}}{k_{rw}} \dots\dots\dots(10)$$

$$\text{Water, Bbl/MMCFG} = \frac{\text{Reservoir Volume MMCFG}}{\text{Gas:Water}} \times 0.178 \dots\dots\dots(11)$$

Presentation of Data and Results

Oil Reservoir, Kentucky

Eleven wells were analyzed from a carbonate and sand sequence in Kentucky. Productive reservoirs are mostly thin columns of oil overlying much thicker wet zones. A total of twelve tests (lettered A through K on **Fig. 5** and Table 1) were available for analysis. For each perforated interval, initial oil and water test rates are available, from which test water cut can be calculated. Water cut was determined from petrophysical analysis for each of the tested perforated intervals, and compared with test data in Table 1 and Fig. 5. There is very good correlation between actual water produced and petrophysically estimated water cut with the exception of test E from Oil Well 4 and test K from Oil Well 12. **Figs 6a through 9b** show analysis output data and $\log \phi_E$ vs. $\log S_{we}$ cross plots for Oil Well 2, Oil Well 3, Oil Well 6, and Oil Well 9. Appendix A is a detailed description of the data presented on the output template.

Gas Reservoir, NW Colorado

Two wells from a gas reservoir in NW Colorado were analyzed. Gas Well 1 produces small volumes of water – no more than 10 Bbl/MMCFG. Gas Well 2 produces much larger volumes of water – 60-80 Bbl/MMCFG. Table 2 is a comparison of the Bbl/MMCFG, by interval, for each well. The data might suggest that the water being produced in Gas Well 1 is primarily water of condensation. For Gas Well 2, it appears that the water is coming mostly from the lowermost perforated interval. **Figs 10a through 11b** show analysis output data and the $\log \phi_E$ vs. $\log S_{we}$ cross plots for both wells. Appendix B is a detailed description of the data presented on the output template.

Conclusions

1. A petrophysical model is presented to generate continuous curves of relative and effective permeabilities to both wetting and non-wetting phases in hydrocarbon systems. The methodology is based on generating petrophysically-defined depth profiles of permeability, irreducible water saturation, actual water saturation, relative permeability, and effective permeability.
2. The model should be calibrated to specific reservoir measured relative permeability curves.
3. By incorporating fluid viscosities, and for gas reservoirs the appropriate formation volume factor, estimates can be made for water cut for oil reservoirs, and water production in barrels per MMCFG for gas reservoirs.

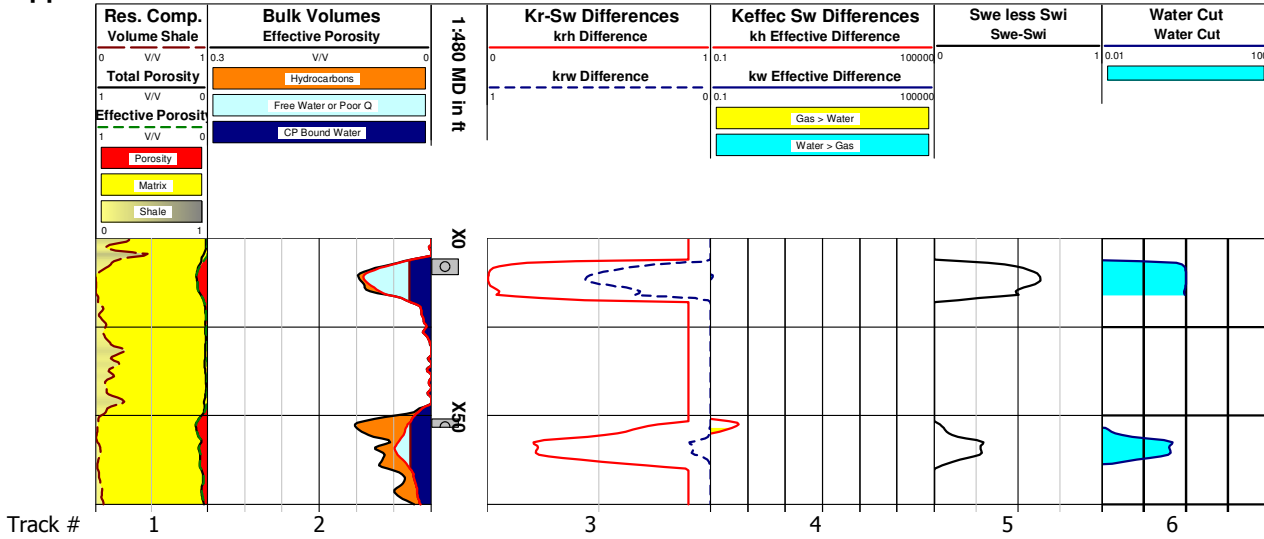
Nomenclature

- ϕ = porosity, %
 k = permeability (effective), mD
 S_{wi} = irreducible water saturation, %
 k_r = relative permeability, mD
 S_w = water saturation, %
 k_{rw} = relative permeability water-wetting phase, mD
 k_{rh} = relative permeability hydrocarbon-wetting phase, mD
 k_w = permeability (effective) water-wetting phase, mD
 k_h = permeability (effective) hydrocarbon-wetting phase, mD

References

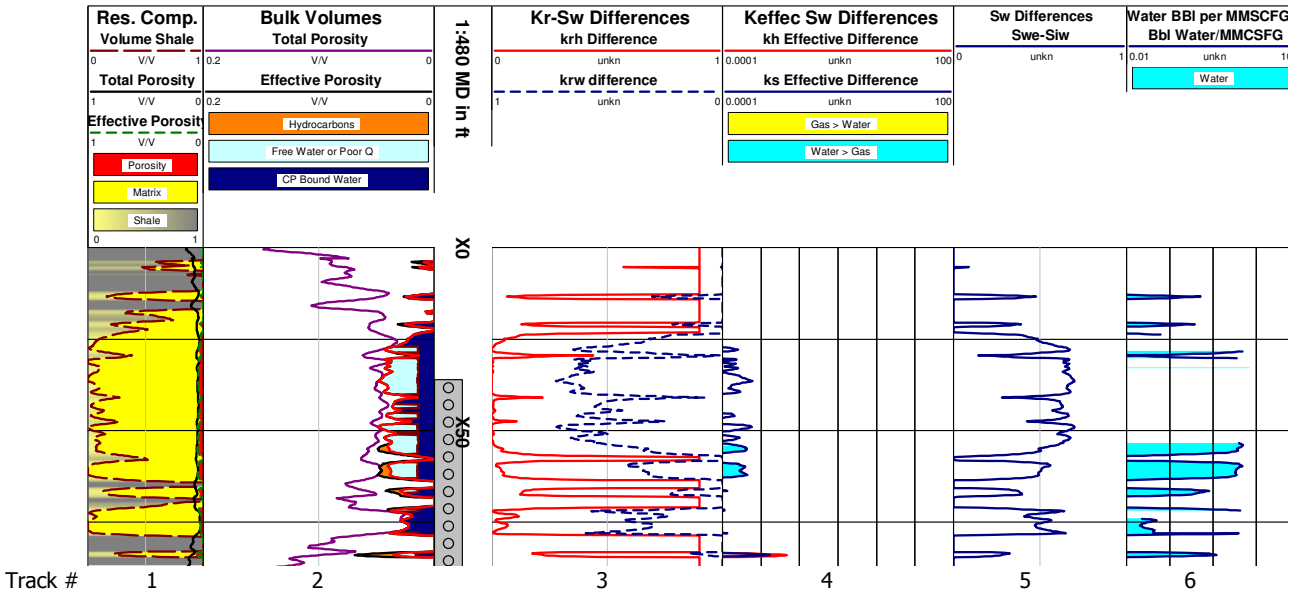
- Buckles, R. S., 1965. Correlating and averaging connate water saturation data. *Journal of Canadian Petroleum Technology* **9** (1): 42-52.
 Burdine, N.T., Gournay, L.S., and Reichertz, P.P., 1950. Pore Size Distribution of Reservoir Rocks. *Journal of Petroleum Technology* **2** (7): 195-204.
 Craft, B.C. and Hawkins, M.F. 1959. *Applied Petroleum Reservoir Engineering*. New Jersey: Prentice-Hall.
 Holmes, M., Holmes, A., and Holmes, D., 2009. Relationship Between Porosity and Water Saturation: Methodology to Distinguish Mobile from Capillary Bound Water. Oral presentation given at the 2009 AAPG ACE, Denver, Colorado 7-10 June.
 Timur, A., 1968. An Investigation of Permeability, Porosity, and Residual Water Saturation Relationships. In *Transactions of the SPWLA Ninth Annual Logging Symposium, 23-26 June, 1968, New Orleans, Louisiana, USA*, Paper J.

Appendix



Track #	Description of data presented in track
1	Reservoir composition: grey = shale; yellow = matrix; red = porosity
2	Bulk fluid volumes: brown = hydrocarbons; light blue = free water; dark blue = capillary bound water
3	Relative permeabilities: Difference ($S_w - S_{wi}$) model
4	Effective permeabilities: Difference ($S_w - S_{wi}$) model
5	$S_{we} - S_{wi}$
6	Water cut

Appendix A, description of data presented for oil wells



Track #	Description of data presented in track
1	Reservoir composition: grey = shale; yellow = matrix; red = porosity
2	Bulk fluid volumes: brown = hydrocarbons; light blue = free water; dark blue = capillary bound water
3	Relative permeabilities: Difference ($S_w - S_{wi}$) model
4	Effective permeabilities: Difference ($S_w - S_{wi}$) model
5	$S_{we} - S_{wi}$
6	Water production Bbl/MMCSFG

Appendix B, description of data presented for gas wells

Tables

Well	Test	Water Cut from Test, %	Water Cut Estimate from Petrophysics, %
Oil Well 1	A	49	48
Oil Well 2	B	37	25
Oil Well 3	C	0	0
Oil Well 3	D	0	0
Oil Well 4*	E	0	60
Oil Well 5	F	0	10
Oil Well 6	G	50	60
Oil Well 7	H	0	0
Oil Well 9	I	50	30
Oil Well 11	J	80	73
Oil Well 12*	K	82	20
Oil Well 13	L	0	1

Table 1, *Oil Well 4 and Oil Well 12 are the only two wells that do not show good correlation between actual and petrophysically estimated water cut.

Perforation	Gas Well 1		Gas Well 2	
	Interval, ft	Water, Bbl/MMCFG	Interval, ft	Water, Bbl/MMCFG
1	4722-5042	1.1	5989-6252	46.7
2	5122-5195	0.08	6310-6445	21.7
3	5242-5382	2.0	6636-6745	22.1
4	5459-5642	19.4	6820-6980	491
5	5850-6010	0.1	7065-7255	6.6
6	6040-6210	0.1	7340-7495	4.6
7	6452-6350	0.4	7610-7812	8.4
8	6581-6809	2.4	7948-8200	13.2
9	--	--	8305-8710	18.8
10	--	--	8894-9220	561
Total		3.3		46.7

Table 2

Figures

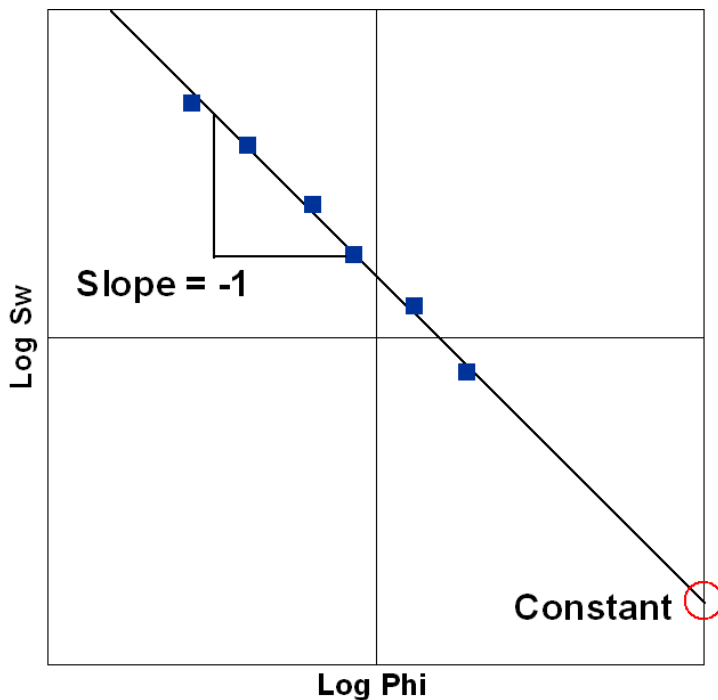


Figure 1, example $\log \phi$ vs. $\log S_w$ from Eq. 1

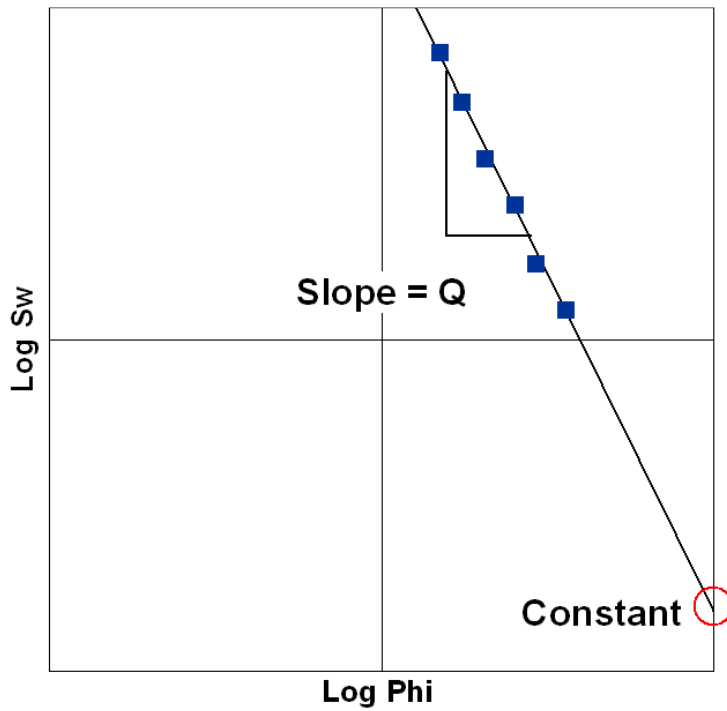


Figure 2, example $\log \phi$ vs. $\log S_w$ from Eq. 2

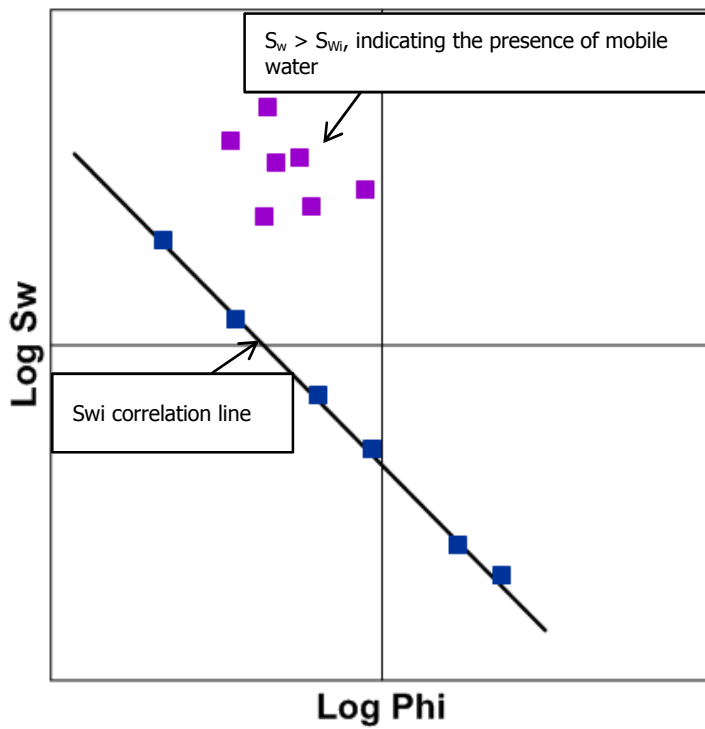


Figure 3, example $\log \phi$ vs. $\log S_w$, showing data points where $S_w > S_{wi}$, which indicates the presence of mobile water

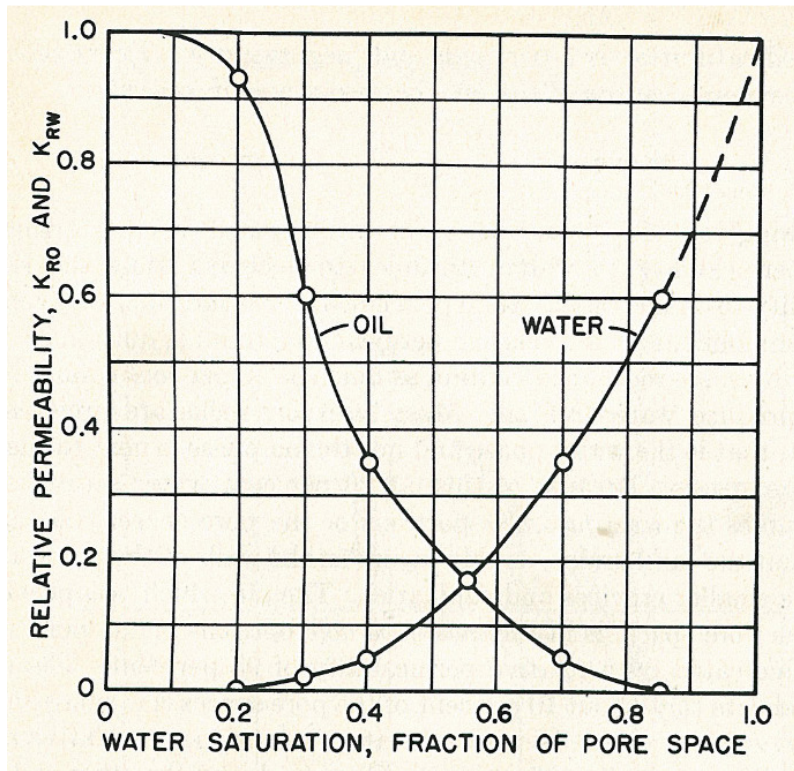


Figure 4, example relative permeability curve (Craft and Hawkins, 1959)

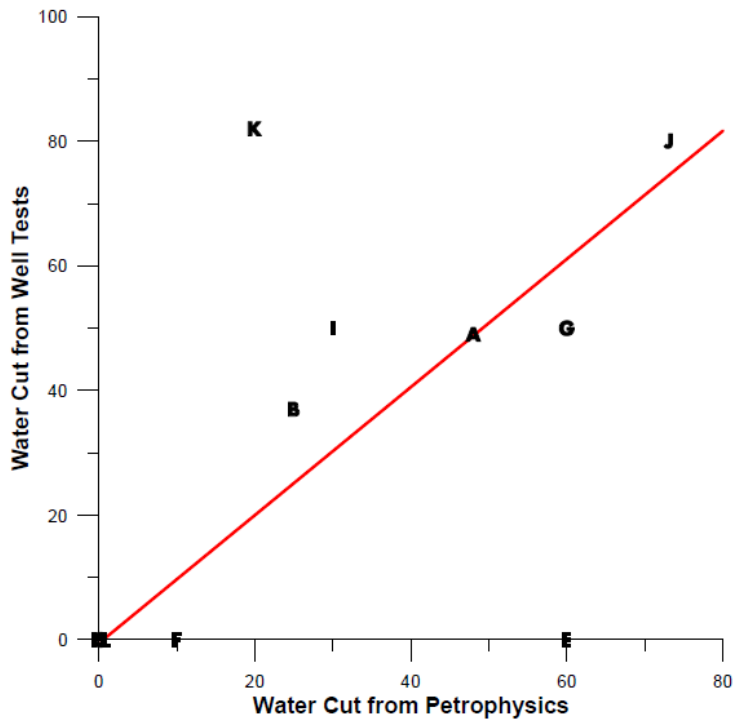


Figure 5, water cut from tests vs. water cut estimated from petrophysics. All wells show good correlation except test E from Oil Well 4, and test K from Oil Well 12.

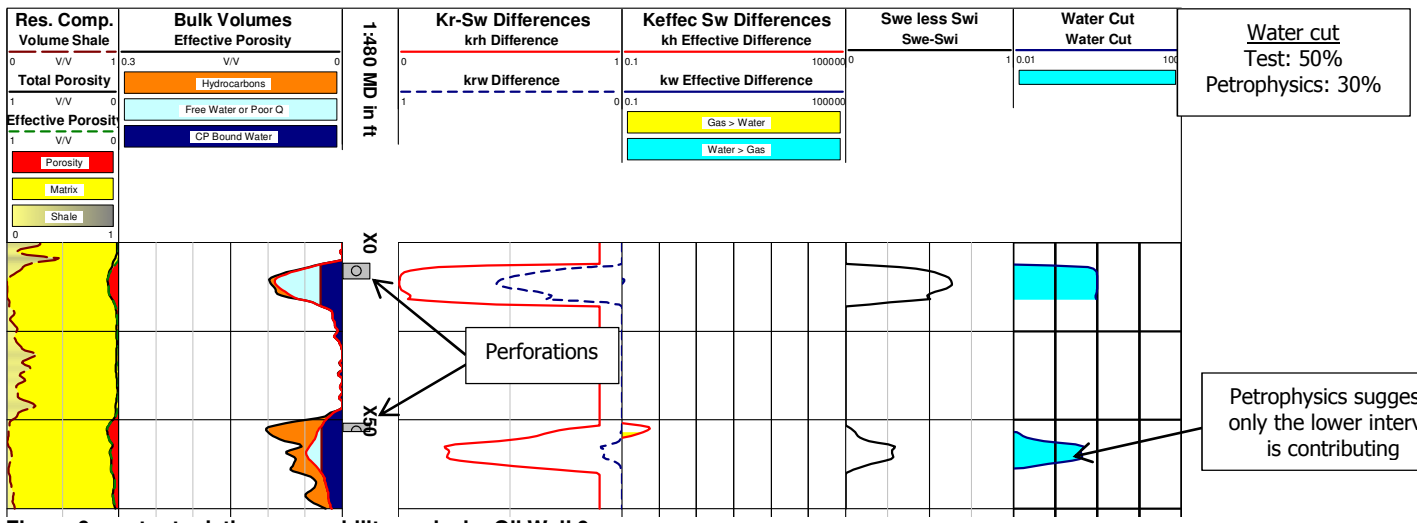


Figure 6a, output relative permeability analysis, Oil Well 9

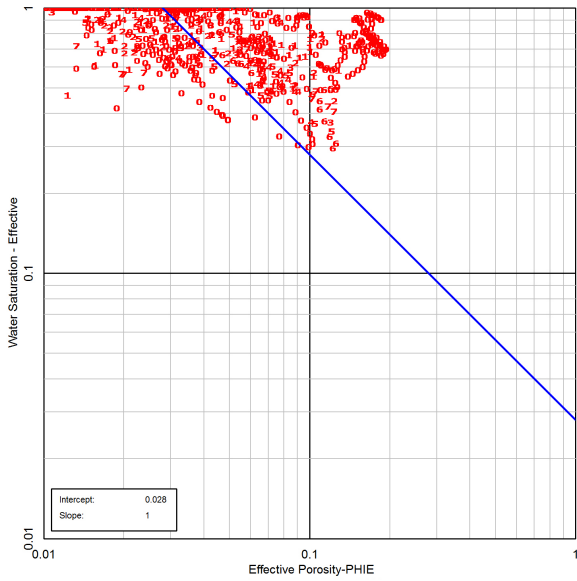


Figure 6b, ϕ_E vs. S_{we} , Oil Well 9

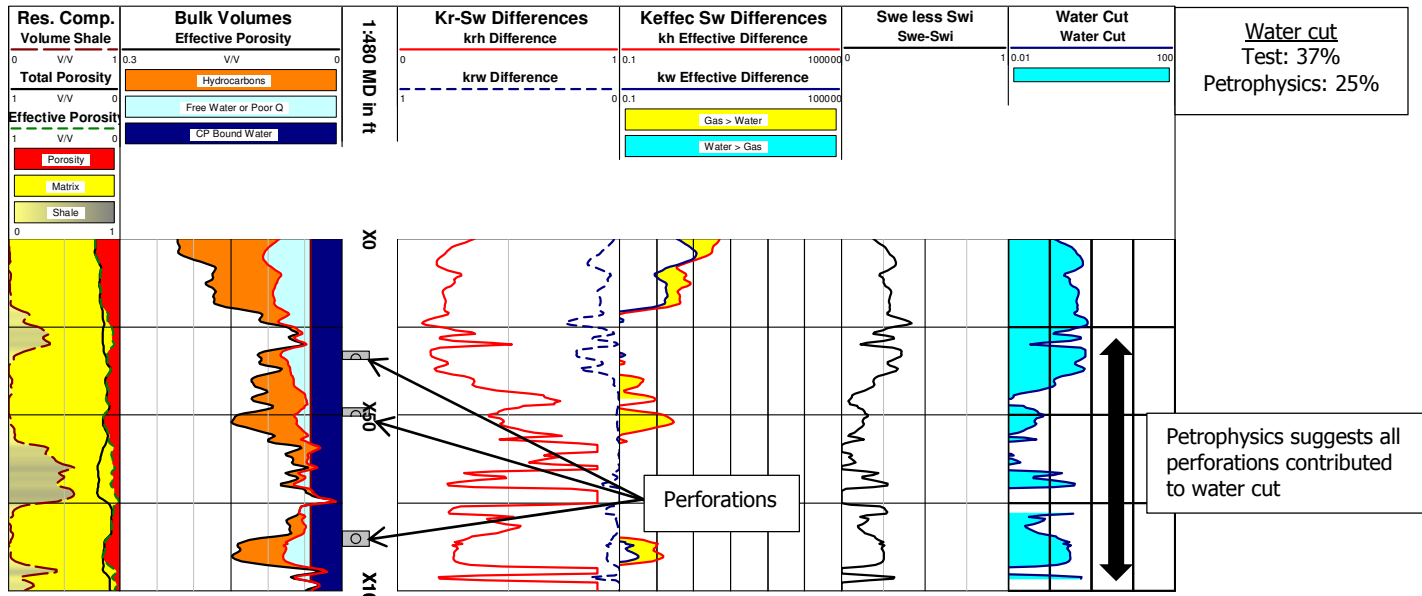


Figure 7a, output relative permeability analysis, Oil Well 2

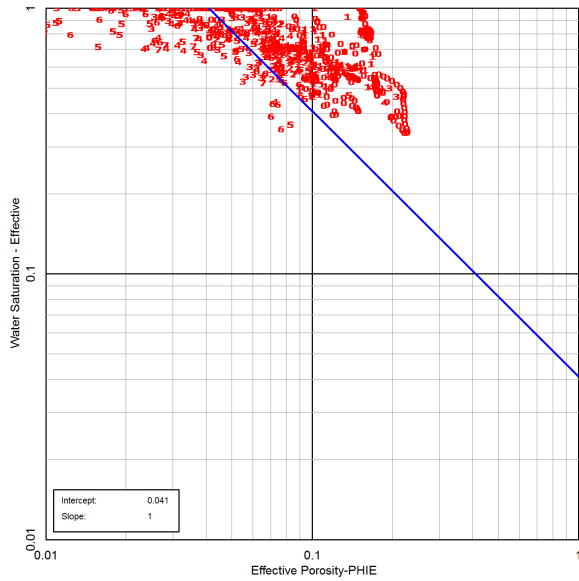


Figure 7b, ϕ_E vs. S_{we} Oil Well 2

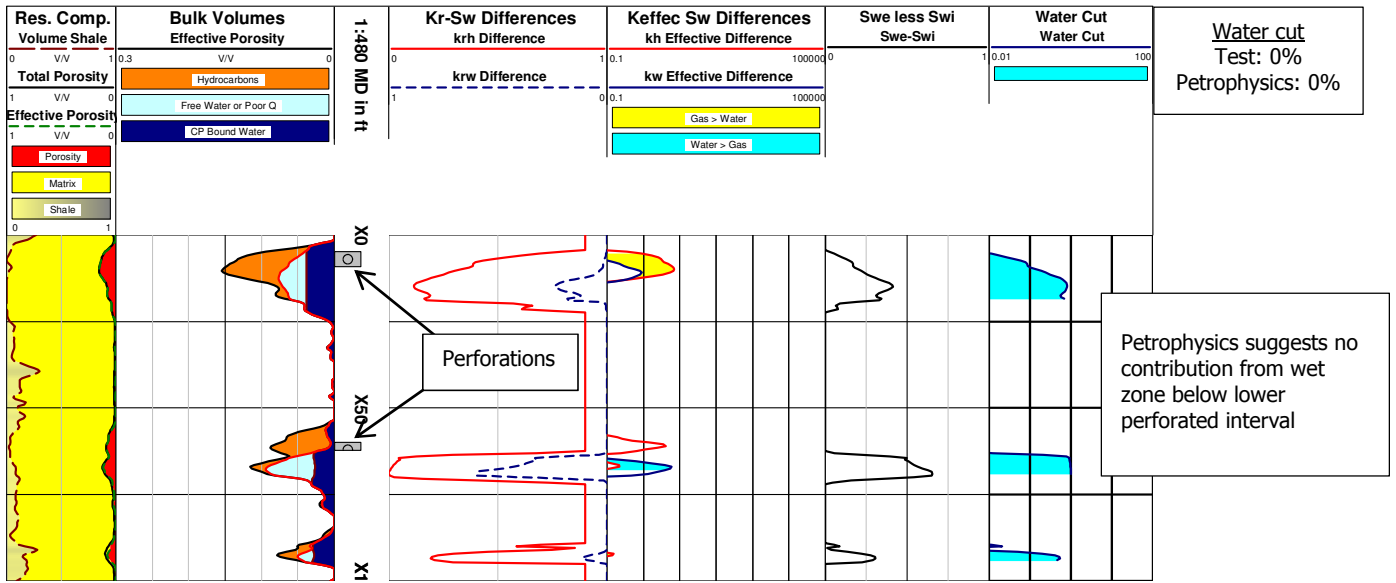


Figure 8a, output relative permeability analysis, Oil Well 3

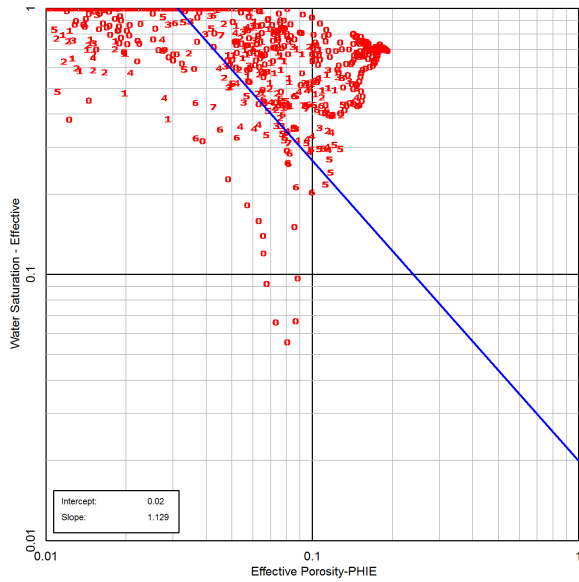


Figure 8b, ϕ_E vs. S_{we} , Oil Well 3

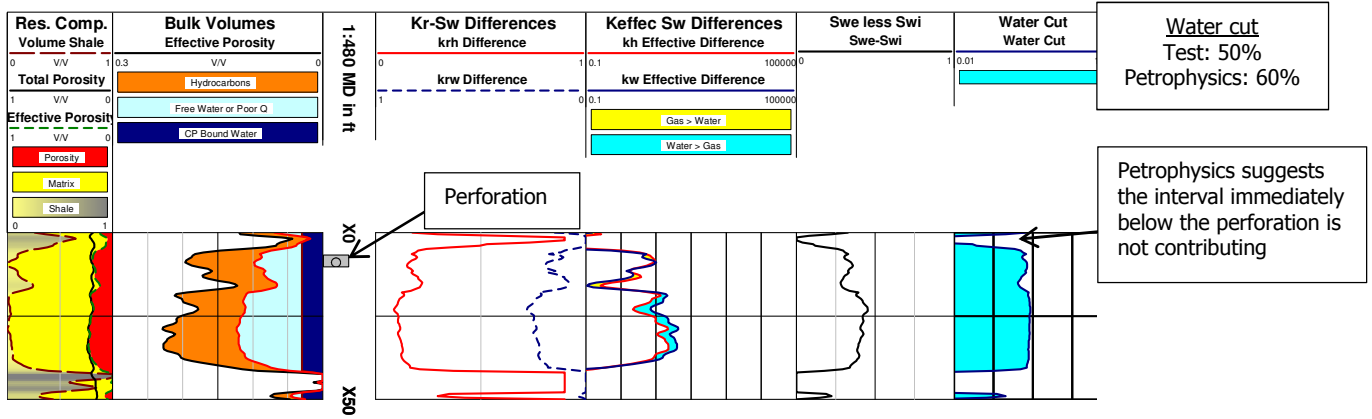


Figure 9a, output relative permeability analysis, Oil Well 6

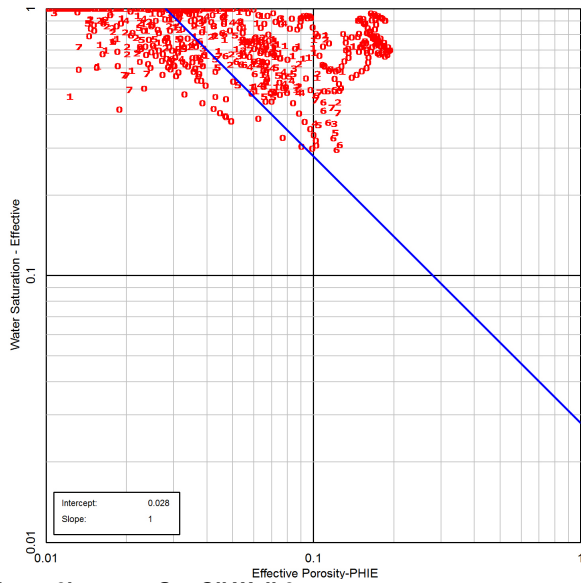


Figure 9b, ϕ_E vs. S_{we} , Oil Well 6

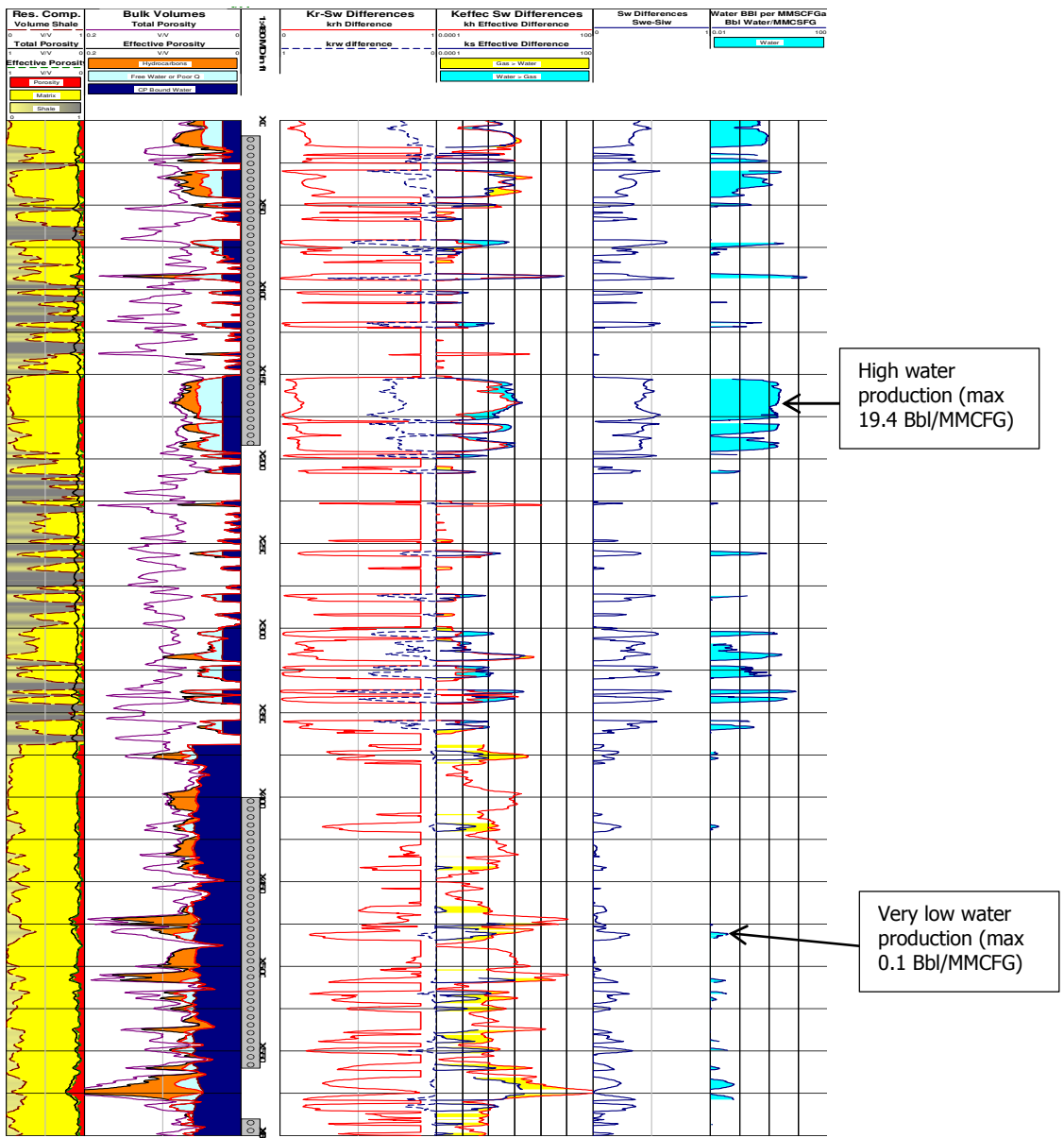


Figure 10a output relative permeability analysis, Gas Well 1

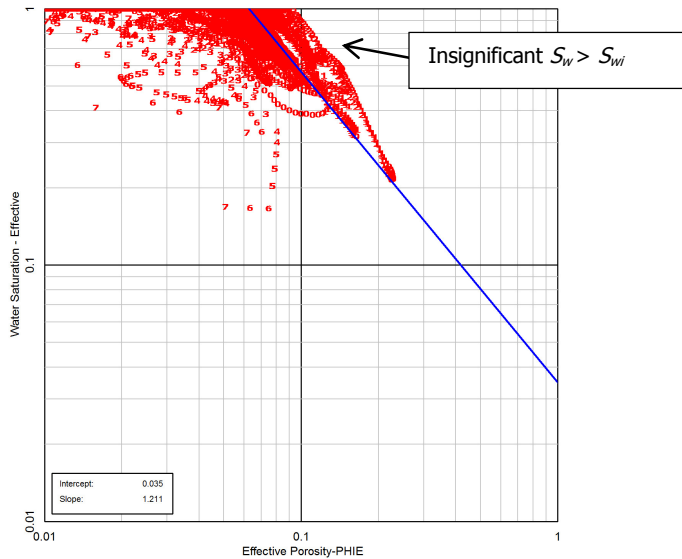


Figure 10b, ϕ_E vs. S_{we} , Gas Well 1

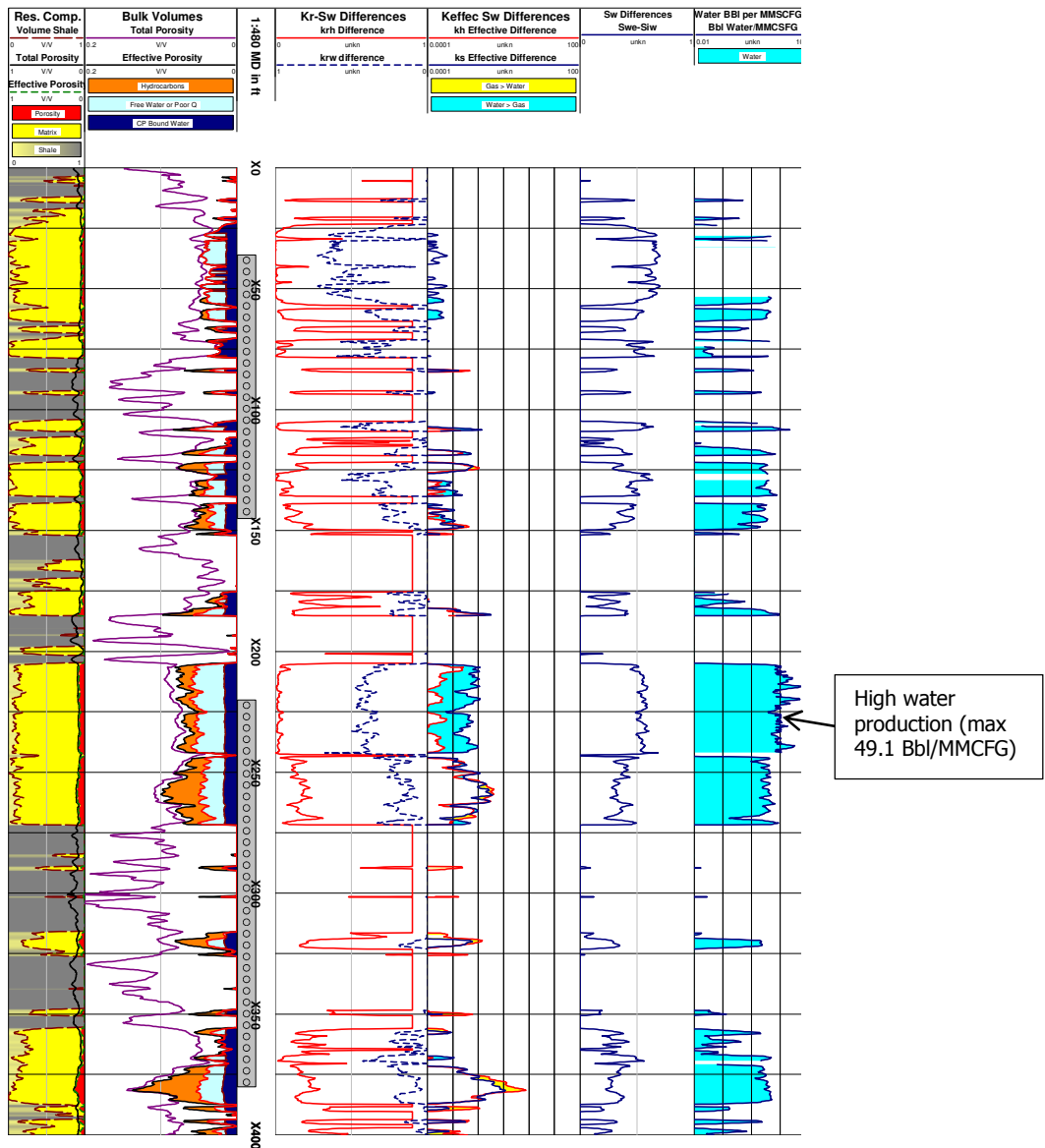


Figure 11a output relative permeability analysis, Gas Well 2

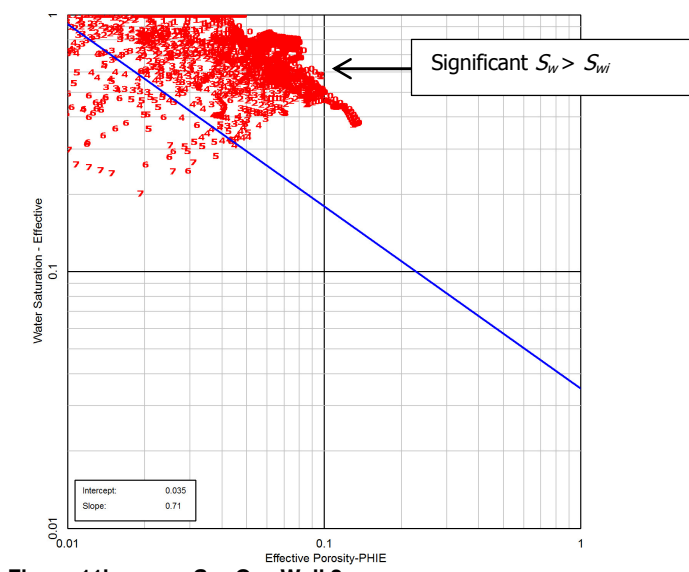


Figure 11b, ϕ_E vs. S_{we} , Gas Well 2